

OPTIMIZED GOODMAN DIAGRAM FOR THE ANALYSIS OF FIBERGLASS COMPOSITES USED IN WIND TURBINE BLADES*

Herbert J. Sutherland[†]
Sandia National Laboratories[‡], Albuquerque, NM 87185-070

and

John F. Mandell[§]
Montana State University, Bozeman, MT 59717

Mandell, et al have recently presented an updated Goodman diagram for a fiberglass composite that is a typical wind turbine blade material. Their formulation uses the MSU/DOE Fatigue Data Base to develop a Goodman diagram with detailed S-N information at thirteen R-values. This diagram is the most detailed to date, and it includes several loading conditions that have been poorly represented in earlier studies. Sutherland and Mandell have used this formulation to analyze typical loads data from operating wind farms and the failure of coupons subjected to spectral loading. The detailed Goodman diagram used in these analyses requires a significant investment in materials testing that is usually outside the bounds of typical design standards for wind turbine blades. Thus, the question has become: How many S-N curves are required for the construction of a Goodman diagram that is sufficient for an “accurate” prediction of equivalent fatigue loads and service lifetimes? To answer this question, the loads data from two operating wind turbines and the failure of coupons tested using the WISPERX spectra are analyzed using both a linear and a non-linear damage model. For the analysis, the predicted service lifetimes that are based on the Goodman diagram constructed from 13 R-values are compared to the predictions for Goodman diagrams constructed with fewer R-values. The results illustrate the optimum number of R-values is 5 with them concentrated between R-values of -2 and 0.5 , or -2 and 0.7 .

Nomenclature

N	=	Mean number of constant-amplitude cycles to failure
N_0	=	Fitting parameter
$N_{95/95}$	=	With a 95 percent level of confidence, the material will meet or exceed this design value for the number of constant-amplitude cycles to failure 95 percent of the time
R	=	R-value of the fatigue cycle
T	=	Time
D	=	Damage
L	=	Lifetime
a, b, c	=	Fitting parameters
i, j, k, l	=	indexes
σ	=	Applied stress

* This paper is declared a work of the U.S. Government and is not subject to copyright protection in the United States.

[†] DMTS, Wind Energy Technology Department, MS-0708, ASME Fellow.

[‡] Sandia is a multiprogram laboratory operated by Sandia Corporation, a Lockheed Martin company, for the U.S. Department of Energy under contract DE-AC04-94AL85000.

[§] Professor of Chemical Engineering, 302 Cableigh Hall.

σ_a	=	Amplitude of the stress cycle
σ_m	=	Mean stress of the fatigue cycle
σ_{\min}	=	Minimum stress of the fatigue cycle
σ_{\max}	=	Maximum stress of the fatigue cycle
σ_O	=	Ultimate tensile or compressive strength
σ_R	=	Residual strength

I. Introduction

The damage analysis of wind turbine blades requires a detailed description of the fatigue load spectra and the fatigue behavior of the blade material. The latter is typically presented as a Goodman diagram in which the cycles-to-failure (S-N data) are plotted as a function of mean stress and range along lines of constant R-values.¹ The R-value for a fatigue cycle is defined as:

$$R = \frac{\sigma_{\min}}{\sigma_{\max}}, \quad (1)$$

where σ_{\min} is the minimum stress and σ_{\max} is the maximum stress in a fatigue stress cycle (tension is considered positive and compression is negative).

Mandell, et al² have recently presented an updated Goodman diagram for a fiberglass composite that is a typical wind turbine blade material. Their formulation uses the MSU/DOE Fatigue Data Base³ to develop a Goodman diagram with detailed information at thirteen R-values. This diagram is the most detailed to date, and it includes several loading conditions that have been poorly represented in earlier studies.

Sutherland and Mandell have used this formulation to analyze typical loads data from operating wind farms⁴ and the failure of coupons subjected to spectral loading.^{5,6} The results of the former illustrate a significant overestimation of the equivalent fatigue loads when the mean stress is not considered in the calculation. And, that the updated Goodman diagram predicts a significant difference in accumulated damage when the Goodman diagram includes information on the transition between compressive and tensile failure modes. The analysis of coupon failures under spectral loads illustrates that Miner's rule does not predict failure very well and that nonlinear models can accurately predict failures with an appropriate choice of the nonlinear degradation parameter.

The detailed Goodman diagram used in these analyses requires a significant investment in materials testing that is usually outside the bounds of typical design standards for wind turbine blades. Thus, the question has become: How many R-values curves are required for the construction of a Goodman diagram that is sufficient for an "accurate" prediction of equivalent fatigue loads and service lifetimes. In the analysis presented here, we analyze the loads data from operating wind turbines and from coupon tests with Goodman diagrams of varying degrees of accuracy. The relative accuracy of each is determined by comparing the predicted service lifetimes that are based on the Goodman diagram constructed from 13 R-values to the predictions for Goodman diagrams constructed with fewer R-values.

II. Goodman Diagrams

For the analysis of S-N data, the preferred characterization is the Goodman diagram. In this formulation, the cycles-to-failure are plotted as functions of mean stress σ_m and alternating stress σ_R along lines of constant R-values. Between R-value lines, the constant cycles-to-failure plots are typically, but not always, taken to be straight lines.

The mean diagram² was constructed from thirteen S-N curves that were fit with a three-parameter equation of the following form:

$$\sigma_o - \sigma = a\sigma \left[\frac{\sigma}{\sigma_o} \right]^{-b} (N^c - 1), \quad (2)$$

where σ is the maximum applied stress, σ_o is the ultimate tensile or compressive strength (obtained at a strain rate similar to the 10 Hz fatigue tests), N is the mean number of constant-amplitude cycles to failure, and a, b, and c are the fitting parameters. The results of these fits are summarized in Table I. The resulting "full" Goodman diagram is shown in Fig. 1.

Table I : Parameters for the Thirteen R-Values for Material DD16.

R-Value	Model (Equation 2)			95/95 (Equation 3)
	a	b	c	$\log_{10}(N_o)$
1.1	0.06	3	0.05	4.43
1.43	0.06	3	0.15	1.85
2	0.06	4	0.25	2.67
10	0.1	4	0.35	0.87
-2	0.01	4	0.55	0.59
-1	0.02	3	0.62	0.53
-0.5	0.45	0.85	0.25	0.64
0.1	0.42	0.58	0.18	0.70
0.5	0.075	2.5	0.43	0.79
0.7	0.04	2.5	0.45	0.65
0.8	0.035	2.5	0.4	0.79
0.9	0.06	2.5	0.28	1.20
1*	0.21	3	0.14	3.03

*Assumes a frequency of 10 Hz.

These data were also used to construct the 95/95 Goodman diagram shown in Fig. 2. The 95/95 fit implies that, with a 95 percent level of confidence, the material will meet or exceed this design value 95 percent of the time. For this diagram, the number of cycles to failure is given by:

$$\log_{10}[N_{95/95}] = \log_{10}[N] - \log_{10}[N_o] \quad , \quad (3)$$

where $\log_{10}(N)$ is determined from Eq. 2 and $\log_{10}[N_o]$ is tabulated for each of the thirteen R-values in Table I.

These two diagrams are compared to one another in Fig. 3.

III. Load Spectra

A. Turbine Load Spectra

To evaluate the effects of the various Goodman diagrams on damage calculations requires a detailed knowledge of the load (and stress or strain) spectra.

The LIST (Long-term Inflow and Structural Test) program has obtained long-term load spectra for two turbines. The first is a three-bladed, up-wind Micon 65/13M wind turbine. This turbine is being tested at a USDA site located near Bushland, Texas. This site is representative of most Great Plains commercial sites. For a complete description of the turbine, its instrumentation and the site, see Sutherland, et al.^{7]. Sutherland et al.^{8,9} has reported on other analyses of these data. A typical fatigue load spectrum for edgewise bending for this turbine is shown in Fig. 4.}

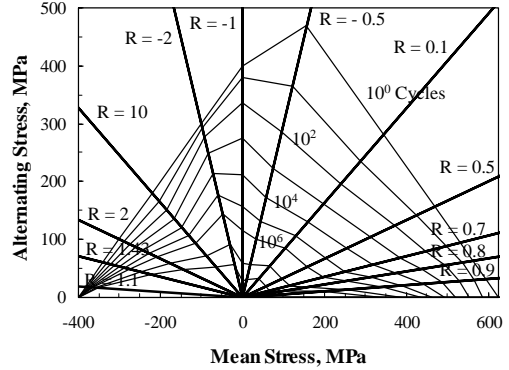


Fig. 1. Mean Goodman Diagram for Database Material DD16, Fit with Eq. 2.

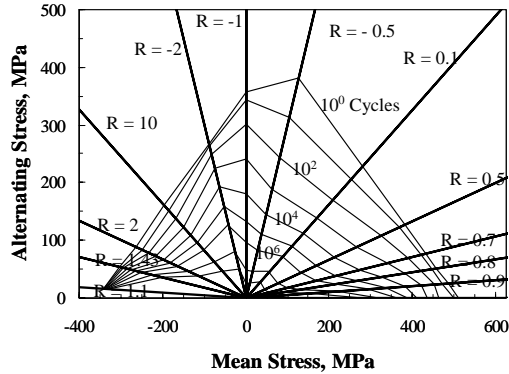


Fig. 2. 95/95 Goodman Diagrams for Database Material DD16, Fit with Eqs. 2 and 3.

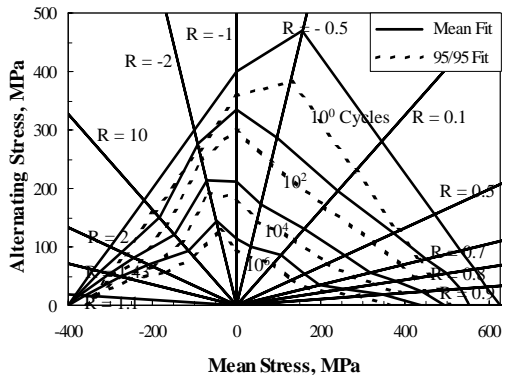


Fig. 3: Comparison of Mean and 95/95 Goodman Diagrams.

The second turbine is the ART (Advanced Research Turbine). It is a Westinghouse 600-kW wind turbine that is currently located at the National Wind Technology Center (NWTC) near Boulder, Colorado. Under the auspices of the LIST program, Kelley et al.¹⁰ collected a long-term data set that includes both the dynamic response of the turbine and detailed inflow measurements. Sutherland, Kelley and Hand¹¹ have reported an analysis of these data. A typical fatigue load spectrum for edgewise bending for this turbine is shown in Fig. 5.

For the two turbine spectra, the cycle counts were determined as a function of wind speed. The wind speed bins for the Bushland turbine were 7-9, 9-11, 11-13, 13-15 and 15-17 and >17 m/s. For the ART, the same wind speed bins were used, except there was no 7-9 m/s bin. Within each wind speed bin, the cycles were binned by mean and range. These bins were combined to form a one-year cycle count matrix, also by mean and range, based on a Rayleigh wind speed distribution with a 6.3 m/s (14 mph) mean. For both turbines, the cut-in wind speed was taken to be 6 m/s and the cut-out wind speed was taken to be 19 m/s. The first wind speed bin is used for all winds between cut-in and the first bin, and the last bin is used for all wind between the last bin and cut-out.

B. Coupon Load Spectrum

Wahl et al.¹² have reported data for the spectral loading of coupons. These data are from coupons that were tested to failure using the WISPERX spectrum¹³. The WISPERX spectrum is the WISPER spectrum with the small amplitude fatigue cycles removed. The WISPERX spectrum, see Fig. 6, consists of over 25,000 peaks-and-valleys (load reversal points) or slightly over 10^4 cycles. The original formulation of the spectrum is in terms of load levels that vary from 0 to 64 with zero at load level 25. When normalized to the maximum load in the spectrum, the load levels take the values shown in the figure. The minimum load level is -0.6923 and, of course, the maximum load level is 1.0.

Figure 6 illustrates that the WISPERX spectrum is primarily a tensile spectrum with a relatively small number of compressive cycles.

Rather than binning the WISPERX spectrum, damage calculations were determined using the mean and range of each cycle.

IV. Damage Calculations

For the analysis presented here, two damage rules have been used: Miner's Rule and Miner's residual strength model. The former is a linear rule that is used on the turbine data and the second is a non-linear rule that is used on the WISPERX data.

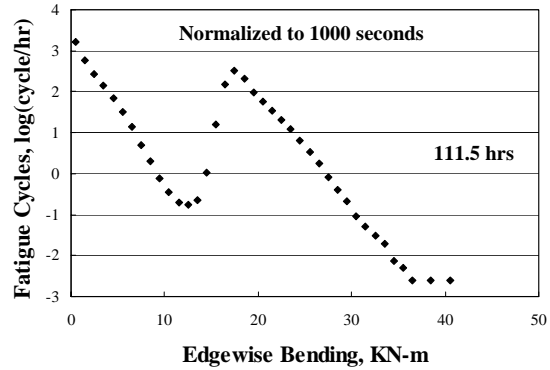


Fig. 4. Edgewise Fatigue Load Spectrum for the 11-13 m/s Wind Speed bin for the Bushland Turbine.

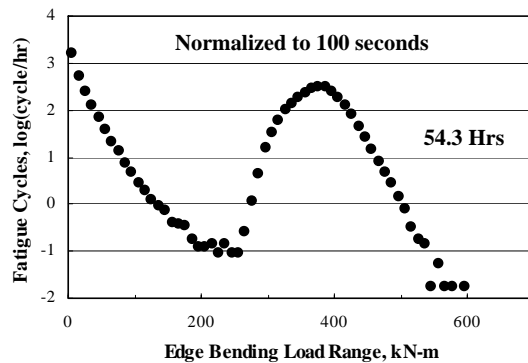


Fig. 5. Typical Fatigue Spectra for Root Bending Moments, >17 m/s Wind Speed Bin for the ART.

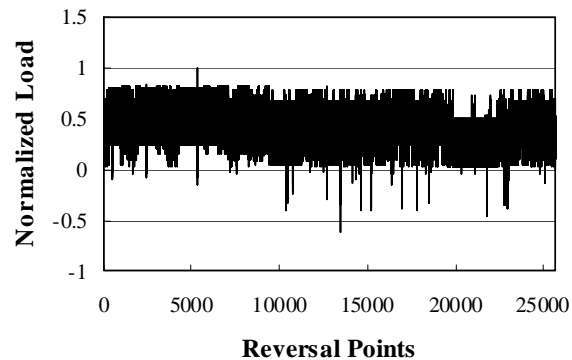


Fig. 6: Normalized WISPERX Spectrum.

A. Miner's Rule

Miner's rule¹ defines the damage \mathbf{D} , predicted for a time interval T , as

$$D = \sum_k \sum_l \frac{n_{kl}(\sigma_m, \sigma_a)}{N(\sigma_m, \sigma_a)} \quad (4)$$

Failure occurs when \mathbf{D} equals one. The predicted service lifetime \mathbf{L} , is the time T required for the damage $\mathbf{D}(T)$ to accumulate to a value of one.

B. Nonlinear Miner's Residual-Strength Model

Miner's rule may also be used to describe the residual strength of composites, see the discussion by Wahl et al.¹² In its general form, the nonlinear Miner's residual-strength model has the following form:

$$\left[\frac{\sigma_R}{\sigma_o} \right]_i = 1 + \left[\frac{\sigma_i - \sigma_o}{\sigma_o} \right] \sum_{j=1}^i \left[\frac{n_j}{N_j} \right]^v, \quad (5)$$

where $[\sigma_R/\sigma_o]$ is the ratio of the residual strength to the static strength σ_o after step i and the exponent v is the nonlinear degradation parameter. Failure occurs when the current value of the residual strength $(\sigma_R)_i$ is exceeded by the $(i+1)$ cycle. The value of v was taken to be 0.85 (Ref. 6).

V. Analysis

The full Goodman diagrams and the two damage laws were used to determine the damage for the cycles in each of load spectra. The damage is then sorted by R-value to determine which ones are the most important. The 13 R-values from the full Goodman diagram were used in this binning process. Based on these results, a "depleted" Goodman diagram is constructed from fewer S-N curves. Predicted service lifetimes from the full and the depleted Goodman diagrams are compared to one another to determine the minimum number of R-values required to obtain the same (within 0.5 percent of each other) predicted service lifetime. Both the mean and the 95/95 S-N curves were analyzed.

A. Turbine Spectra

For the two turbine load spectra, the annual number of cycles by range and mean was determined first, see Fig. 7. The damage** was then determined for each bin, see Fig. 8. These damage estimates were then re-binned by R-value and range, see Fig. 9. Based on the distribution of damage, the Goodman diagram was reduced to a selected set of R-values. Damage estimates (predicted service lifetime) were then recomputed and

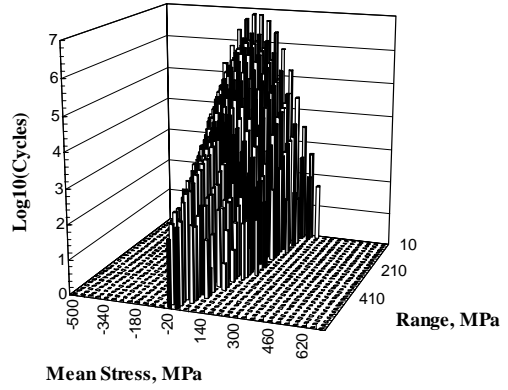


Fig. 7: Annual Flapwise Bending Cycles for the Bushland Turbine.

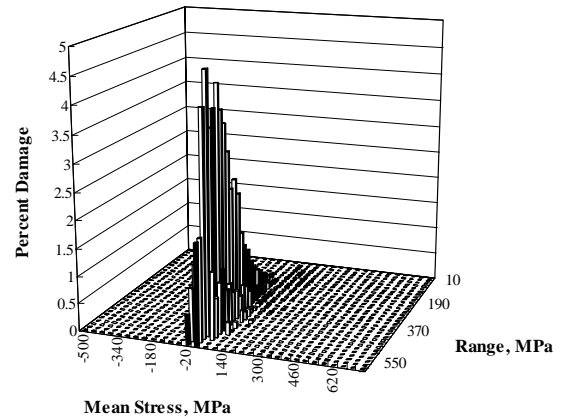


Fig. 8: Annual Damage Estimates for the Bushland Turbine on the Tension Bending Side of the Blade.

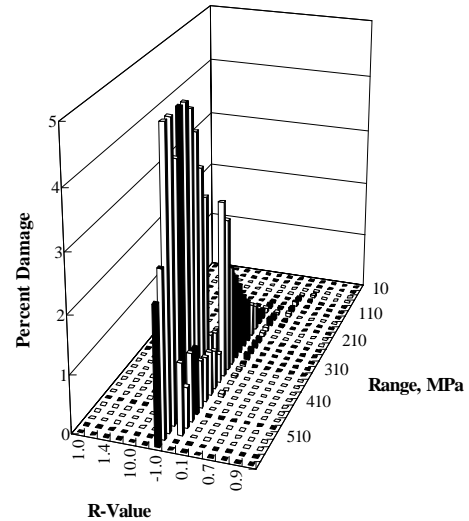


Fig. 9: Annual Damage Estimates for the Bushland Turbine on the Tension Bending Side of the Blade.

** For the residual strength model, the "damage" in the fractional loss of residual strength defined by the last term of Eq. 5.

the results compared with the original prediction.

The approach for constructing the Goodman diagrams from less than 13 S-N curves, started by choosing the minimum number of adjacent S-N curves that could cover most of the damage. The number of S-N curves was then expanded by adding adjacent S-N curves to the sequence. Once the number of S-N curves was determined that produced the same service lifetime prediction as the 13 S-N curve Goodman diagram, selected S-N curves were removed from the sequence

The results of these analyses are summarized in Figs. 10 and 11 and Table II for the Bushland turbine and in Figs. 12 and 13 and Table III for the ART. In these tables, the number of R-values used in the construction of the Goodman diagram is shown in the column labels. For sequential R-values (taken from the original 13 R-values), the label is a single number. For non-sequential R-values, a letter (a or b) is added to the number of S-N curves. The actual R-values used in each column are listed below each table.

1. *Bushland Turbine*

While the load spectra for the Bushland turbine contains loads in all 13 R-value bins, see the discussion by Mandell et al.,² the damage is concentrated as shown in Figs. 10 and 11 (Note that Fig. 11 is a 2-D plot of Fig. 9, where the damage has been summed along constant R-value lines).

As shown in these figures, the spectra on the edgewise-bending side, are concentrated between R-values of -2 and 0.5 . Thus, a Goodman diagram containing 5 S-N curves at R-values of -2 , -1 , -0.5 , 0.1 and 0.5 should predict the failure lifetime accurately. As summarized in Table II (see the rows labeled Edge under the column labeled 5), this formulation of the Goodman diagram yields service life predictions that are within 0.5 percent of those predicted by the full Goodman.

The flapwise bending spectra has a wider range of important R-values, see Figs. 10 and 11. At least 7 and maybe nine S-N curves will be required for an accurate estimate of the service lifetime. As shown in Table II, 7 S-N curves with R-values are required to accurately predict the service lifetime (see the column labeled 7). If the $R=10$ S-N curve is removed (see the column labeled 6), the predictions are within 1 percent. If the $R=0.7$ S-N curve is removed, the difference increases to 16 percent (see the column labeled 5), but this difference can be reduced to 8 percent by removing the $R=0.5$ S-N curve instead (see the column labeled 5a). Reducing the number of S-N curves any further yields unacceptable predictions that are as much as a factor of 3 low or 2.5 high (see the columns labeled 4 and 4a).

Thus, for the Bushland spectra, a Goodman diagram constructed from 6 S-N curves at R-values of -2 , -1 , -0.5 , 0.1 , 0.5 and 0.7 predicts the service lifetime within 1 percent. And one constructed from 5 R-values curves yields predictions within 8 or 16 percent.

Similar results were obtained for the 95/95 S-N curves. For the 6 S-N curve Goodman-diagram, the predictions were also within 1 percent and for the 5 S-N curve, the predictions were within 15 percent.

2. *ART*

A similar analysis was conducted for the ART. As shown in Figs. 12 and 13 and summarized in Table III, the breath of the cycles for this turbine are significantly less than for the Bushland turbine. A Goodman diagram constructed from as little as 5 S-N curves predicts the service lifetime within 0.5 percent for the compression bending side. With 4 R-value curves, the predictions are within 2 percent. For 3 R-value the predictions deteriorate to 34 percent.

Similar results were obtained for the tensile bending side. For the 4 S-N curve Goodman diagram, the predictions were also within 1 percent and for the 3 S-N curve Goodman diagram, the predictions were within 35 percent.

B. WISPERX Spectrum

The analysis of the WISPERX spectrum was conducted in the same manner as for the turbine spectra except that the WISPERX spectrum was used directly, without a conversion to an annual distribution. As illustrated previously,⁵ the linear damage model does not predict the failure very well, while the non-linear model accurately predicts failure when the fatigue exponent is chosen properly. Therefore, only the non-linear model will be considered here.

The WISPERX coupon data are unique when compared to turbine spectra in that the failure data are available at various load levels,¹² see Fig. 14. Goodman diagrams constructed from various S-N curves were used to predict the failures for the entire range of the data.

As illustrated by Fig. 6, the WISPERX spectrum is primarily a tensile spectra. The damage estimate for the WISPERX spectrum, see Fig. 15, illustrates this observation as well, with more than 90 percent of the damage concentrate in the R-value bins of 0.1 and 0.5 .

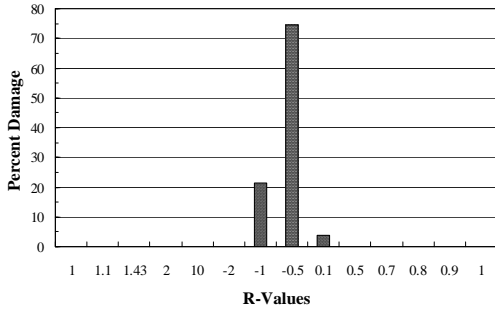


Fig. 10a: Damage in the Edgewise Bending Direction.

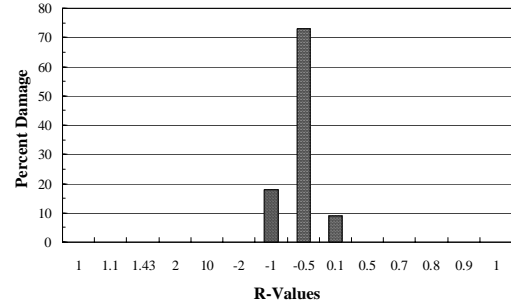


Fig. 11a: Damage in the Edgewise Bending Direction.

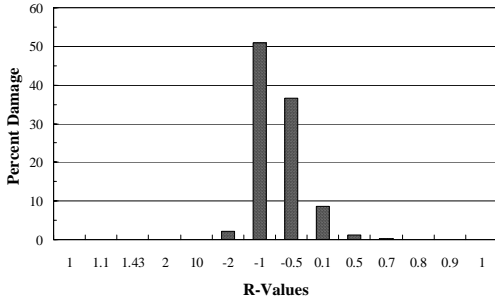


Fig. 10b: Damage in the Flapwise Bending Direction.

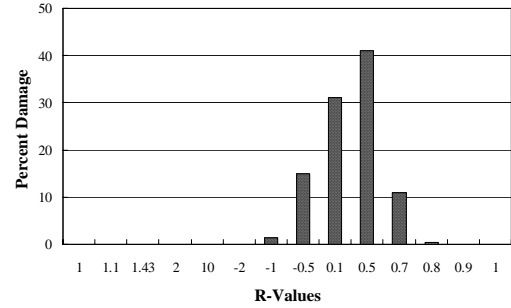


Fig. 11b: Damage in the Flapwise Bending Direction.

Fig. 10: Damage Estimates for the Bushland Turbine on the Compression Bending Side of the Blade using the Full Mean Goodman Diagram.

Fig. 11: Damage Estimates for the Bushland Turbine on the Tension Bending Side of the Blade using the Full Mean Goodman Diagram.

Table II. Normalized Service Lifetime for the Bushland Turbine Using Various Goodman Diagrams and Mean S-N Curves.

R-Values Used*	Full Goodman	3	4	4a	5	5a	6	6a	6b	7
LINEAR DAMAGE MODEL										
Compression										
Edge	100	86	100	74	100	100	100	100	93	100
Flap	100	19	102	62	100	100	99	100	59	100
Tension										
Edge	100	99	100	66	100	100	100	100	99	100
Flap	100	243	254	33	116	108	100	108	99	100
NON-LINEAR DAMAGE MODEL										
Compression										
Edge	100	85	100	77	100	100	100	100	92	100
Flap	100	22	102	64	100	100	99	100	61	100
Tension										
Edge	100	99	100	67	100	100	100	100	99	100
Flap	100	220	232	38	116	106	100	106	99	100

*S-N Curves Used to construct the Goodman diagram:

3: -1, -0.5, 0.1

5: -2, -1, -0.5, 0.1, 0.5

6a: 10, -2, -1, -0.5, 0.1, 0.7

4: -2, -1, -0.5, 0.1

5a: -2, -1, -0.5, 0.1, 0.7

6b: 10, -1, -0.5, 0.1, 0.5, 0.7

4a: -2, -1, -0.5, 0.7

6: -2, -1, -0.5, 0.1, 0.5, 0.7

7: 10, -2, -1, -0.5, 0.1, 0.5, 0.7

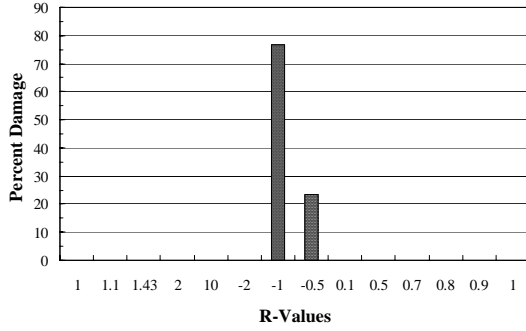


Fig. 12a: Damage in the Edgewise Bending Direction.

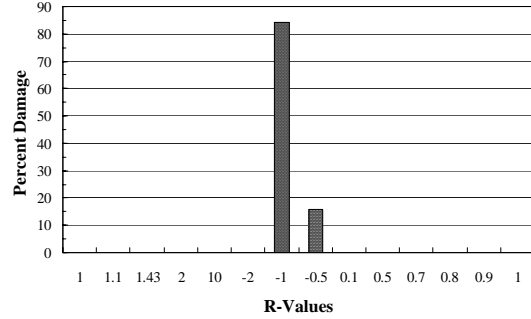


Fig. 13a: Damage in the Edgewise Bending Direction.

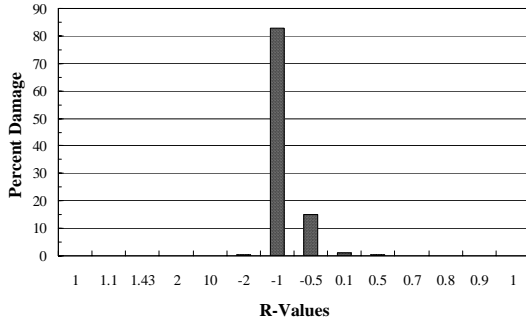


Fig. 12b: Damage in the Flapwise Bending Direction.

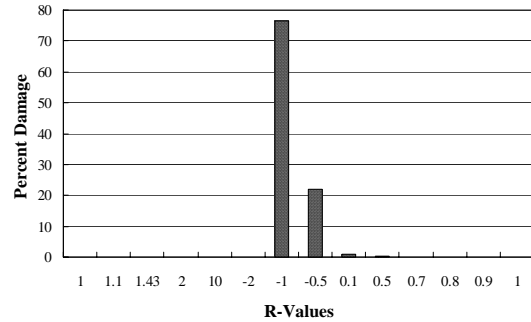


Fig. 13b: Damage in the Flapwise Bending Direction.

Fig. 12: Damage Estimates for the ART on the Compression Bending Side of the Blade using the Full Mean Goodman Diagram.

Fig. 13: Damage Estimates for the ART on the Tension Bending Side of the Blade using the Full Mean Goodman Diagram.

Table III. Normalized Service Lifetime for the ART Using Various Goodman Diagrams and 95/95 S-N Curves.

LINEAR:						NON-LINEAR:				
R-Values Used*	Full Goodman	3	4	5	5a	Full Goodman	3	4	5	5a
Compression										
Edge	100	80	100	100	100	100	82	100	100	100
Flap	100	66	101	100	100	100	67	102	100	100
Tension										
Edge	100	74	100	100	100	100	77	100	100	100
Flap	100	82	101	100	100	100	81	101	100	100

*S-N Curves Used to construct the Goodman diagram:

3: -1, -0.5, 0.1 5: -2, -1, -0.5, 0.1, 0.5
 4: -2, -1, -0.5, 0.1 5a: -2, -1, -0.5, 0.1, 0.7

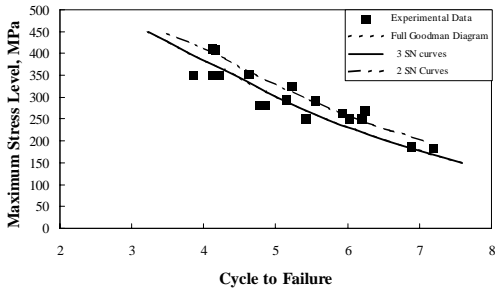


Fig. 14a: Failures Predicted Using the Mean Full Goodman Diagram.

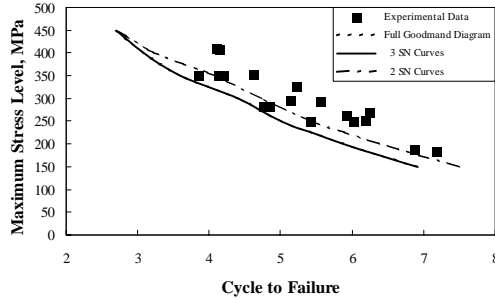


Fig. 14b: Failures Predicted Using the 95/95 Full Goodman Diagram.

Fig. 14: Comparison of Experimental Data to Predicted Failure using Linear Miner's Rule.

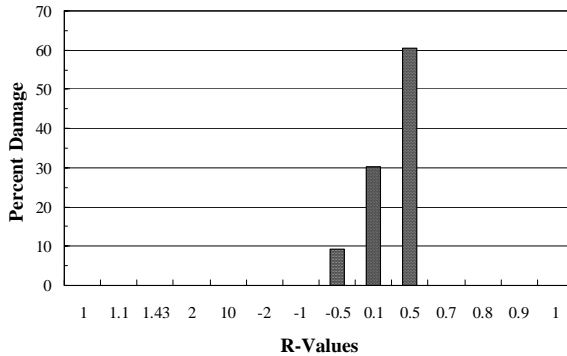


Fig. 15. Damage Estimates for the WISPERX Spectrum using the Full 95/95 Goodman Diagram.

Table IV. Normalized Service Lifetime [$\log(\text{number-of-cycles})$] for the WISPERX Spectrum Using Various Goodman Diagrams and Multipliers.

R-Values Used*	Full Goodman	2	3	3a	3b
Multiplier	95/95				
150	100	108	100	100	101
200	100	109	100	100	101
250	100	109	100	101	102
300	100	107	100	100	101
350	100	113	100	100	102
400	100	105	100	100	102
450	100	101	100	100	100
Multiplier	Mean				
150	100	107	100	100	100
200	100	108	100	100	100
250	100	107	100	100	100
300	100	107	100	100	100
350	100	107	100	100	100
400	100	109	100	100	100
450	100	106	100	100	100

*R-Values: 2 -1, 0.1 3a -1, 0.1, 0.5
3 -0.5, 0.1, 0.5 3b -1, 0.1, 0.7

The failure predictions are summarized in Fig. 14 and in Table IV for the non-linear damage model. In the figure, the lines for the full Goodman diagram and the Goodman diagram constructed from 3 S-N curves lie one-on-top-of-another.

As shown in these predictions, only S-N curves at the -0.5 , 0.1 and 0.5 R-values are required to obtain an accurate prediction of the service lifetime. Even when only the -1 and the 0.1 R-value curves are used, the predictions are within 13 percent of the prediction from the full Goodman diagram.

The distribution of the failure data using the 2 S-N curves Goodman diagram illustrates that the accuracy of the predicted service lifetime is comparatively uniform over all of load levels. There may be a slight

tendency for an increased accuracy, especially using the 95/95 S-N curves, at the higher stress levels, see Fig. 14b.

VI. Summary

As shown in the above discussion, the Goodman diagram constructed from 13 S-N curves can be reduced significantly for the three spectra analyzed here. The three spectra are for a 3-bladed up-wind turbine, a 2-bladed down-wind turbine and the WISPERX test spectrum. The 3-bladed turbine spectra were found to have the largest variation of damage across R-values.

When the Goodman diagram is constructed from R-values of -2, -1, -0.5, 0.1, 0.7, the predictions for the Bushland turbine are within 8 percent, the ART are within 0.5 percent, and the WISPERX are within 2 percent. Using R-values of -2, -1, -0.5, 0.1, 0.5, the predictions for the Bushland turbine are within 16 percent and for the ART and the WISPERX the predictions are within 0.5 percent. Adding the 0.5 or the 0.7 R-value curve to the Goodman diagram raises all predictions to within 0.5 percent. Realizing that the prediction of the service lifetime of a wind turbine is very sensitive to assumptions and computational techniques and that S-N curves are difficult and expensive to obtain, a Goodman diagram constructed from 5 S-N curves, see Fig. 16, is recommended.

Goodman diagrams of other materials of interest (e.g., carbon fiber composites) may differ significantly. Thus, the conclusions reached here are applicable only to materials which are similar in construction to the one used here (fiberglass composite constructed from 0° and $\pm 45^\circ$ fabrics, polyester resin and RTM processing³).

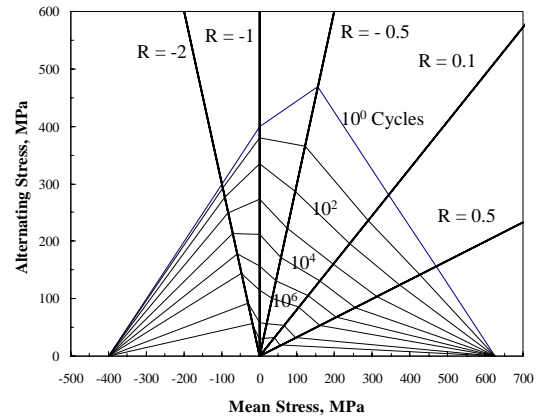


Fig. 16: The Mean Goodman Diagram Recommended for Wind Turbine Spectra.

VII. References

- ¹Sutherland, H.J., 1999, *On the Fatigue Analysis of Wind Turbines*, SAND99-0089, Sandia National Laboratories, Albuquerque, NM, 132 p.
- ²Mandell, J.F., Samborsky, D.D., Wahl, N.K., and Sutherland, H. J., *Testing and Analysis of Low Cost Composite Materials Under Spectrum Loading and High Cycle Fatigue Condition*, ICCM14,
- ³Mandell, J.F., and Samborsky, D.D., *DOE/MSU Composite Material Fatigue Database: Test Methods, Materials, and Analysis*, SAND97-3002, Sandia National Laboratories, Albuquerque, NM (1997).
- ⁴Sutherland, H.J., and Mandell, J.F., "Effect of Mean Stress on the Damage of Wind Turbine Blades," *2004 ASME Wind Energy Symposium*, AIAA/ASME, 2004, pp. 32-44.
- ⁵Sutherland, H.J., and Mandell, J.F., "The Effect of Mean Stress on Damage Predictions for Spectral Loading of Fiberglass Composite Coupons," *EWEA, Special Topic Conference 2004: The Science of Making Torque from the Wind*, 2004, pp. 546-555.
- ⁶Sutherland, H.J., and Mandell, J.F., "The Effect of Mean Stress on Damage Predictions for Spectral Loading of Fiberglass Composite Coupons," *Wind Energy*, in publication.
- ⁷Sutherland, H.J., Jones, P.L., and Neal, B., 2001, "The Long-Term Inflow and Structural Test Program," *2001 ASME Wind Energy Symposium*, AIAA/ASME, pp. 162-172.
- ⁸Sutherland, H.J., "Analysis of the Structural and Inflow Data from the LIST Turbine," *Journal of Solar Energy Engineering*, Transactions of the ASME, v. 124, November, 2002, pp. 432-445.
- ⁹Sutherland, H.J., Zayas, J.R., Sterns A.J., and Neal, B., 2004, "Update of the Long-Term Inflow and Structural Test Program," *2001 ASME Wind Energy Symposium*, AIAA/ASME, in publication.
- ¹⁰Kelley, N., Hand, M., Larwood, S., and McKenna, E., 2002, "The NREL Large-Scale Turbine Inflow and Response Experiment – Preliminary Results," *2002 ASME Wind Energy Symposium*, AIAA/ASME, pp. 412-426.
- ¹¹Sutherland, H.J., Kelley, N.D., and Hand, M.M., "Inflow and Fatigue Response of the NWTC Advanced Research Turbine," *2003 ASME Wind Energy Symposium*, AIAA/ASME, 2003, pp. 214-224.
- ¹²Wahl, N.K., Mandell, J.F., and Samborsky, D.D., *Spectrum Fatigue Lifetime and Residual Strength for Fiberglass Laminates*, Report SAND2002-0546, Sandia National Laboratories, Albuquerque, NM, 2002.
- ¹³Ten Have, A.A., *WISPER and WISPERX: Final Definition of Two Standardized Fatigue Loading Sequences for Wind Turbine Blades*, NLR-TP-1476U, National Aerospace Laboratory NLR, Amsterdam, the Netherlands, 1992.